Chapter 4

Bioimaging and Bio-Sensing Techniques for Lung Cancer Detection

Lulu Wang and Jinzhang Xu

Additional information is available at the end of the chapter

http://dx.doi.org/10.5772/intechopen.72724

Abstract

Early cancer detection and suitable treatment improve the 5-year survival rates of lung cancer significantly. Many cancer diagnostic approaches have been investigated, including mammography, magnetic resonance imaging, ultrasound, computerized tomography, positron emission tomography and biopsy. However, these techniques have some drawbacks such as expensive and time-consuming. Electromagnetic tomography (EMT) has been proposed as a promising diagnostic tool for lung cancer detection. In addition, developing label-free and cost-effective biosensors for target tumor markers detection have attracted attentions worldwide. This chapter reviews the recently developed EMT and bio-sensing techniques for early-stage lung cancer detection.

Keywords: biomedical imaging, biomarker, biosensor, lung cancer, nanoparticles, electromagnetic imaging

1. Introduction

Cancer is a major public health problem worldwide and lung cancer is the leading cause of cancer related deaths [1], which has much lower survival rate than other cancers such as breast cancer [2]. Early diagnosis of cancer is critical, which is expected to contribute significantly to improve the 5-year survival rates [3].

Many medical imaging methods have been intensively investigated for cancer detection, such as computed tomography (CT), magnetic resonance imaging (MRI), positron emission tomography (PET), and ultrasound. They have some drawbacks, such as, expensive and insufficient sensitivity to detect early-stage cancers. CT is the current gold standard medical imaging tool for diagnosis of lung disease, which able to study some features of biological objects such as lesion size, morphological lesion characterization, and follow-up of lesion growth. However, it

Type	Advantage	Disadvantage	Time
Chest X-ray	Reliable	Ionizing radiation, low sensitivity and specificity, sensitivity drops with tissue density increases	Few seconds
CT	Reliable	Expensive, false negative scans, low sensitivity, radiation risks	5 min
MRI	Reliable	Some types of cancers cannot be detected such as ductal and lobular carcinoma, expensive	40–60 min
PET	Reliable	Expensive, need for radioactive substance and sophisticated instrument, not suitable for subjects with other complications	90–240 min

Table 1. Conventional lung screening methods [9].

produces unsafe radiations which may increase cancer risk [4]. To solve this problem, LDCT with lower radiation has been applied for imaging of lung [5]. However, LDCT is associated with high false positive rate (up to 96.4%) [6], this may increase morbidity from unnecessary surgical treatment and also serious psychological burden to the subjects. 18F-Fluorodeoxyglucose PET/CT has been applied in oncological imaging without achieve reliable results [7, 8]. **Table 1** demonstrates the conventional medical imaging methods for lung diseases detection [9].

Recently, electromagnetic tomography (EMT) has been proposed as a promising tool for diagnosis of early-stage diseases such as lung and brain due to its low-cost and high-sensitivity [10].

Biopsy is another common method to distinguish cancerous and benign tissues, but it is expensive and requires trained physicians [11]. Cytokeratin 21-1 (CYFRA21-1) is a sensitive and specific marker for non-small cell lung cancer (NSCLC), especially in squamous cell carcinoma [12]. Biosensors are analytical devices to identify a target sequence by hybridization with complementary probes immobilized on a solid substrate. Biosensors have attracted increased attention due to they have many advantages such as low-cost, easy-to-use and easy to fabricate. Over the past few years, various nanoparticles have been applied to develop biosensors to increase the sensitivity. Other factors affect stability, reproducibility, and sensitivity, including electrode design and probe immobilization. However, biosensor-based approaches are time-consuming and less sensitive for the low marker concentrations at early stages [13]. Therefore, developing a high-sensitivity label-free method for rapid diagnosis of lung diseases is urgently needed.

This paper describes the recent achievements on bio-imaging and bio-sensing approaches for identifying lung cancer. Recent trends in EMT and bio-sensing methods are also reviewed. Several EMT sensor systems, including benefits, limitations, and future research directions are addressed. The rest of this paper is organized as follows: Section 2 describes biomarkers for lung cancer detection; Section 3 reviews biosensor techniques for target lung markers detection; Section 4 presents EMT approaches and measurement systems for imaging of biological tissues; Section 5 presents current trends and future perspectives.

2. Biomarkers for lung cancer detection

Genetic and proteomics-based biomarkers are the two major types of biomarkers, which can be identified in patients through tumor cells, urine, sputum, blood, or other body fluids [14]. **Table 2**

Type	Biomarker
Proteomic biomarkers	Annexin II, APOA1, carcinoembryonic antigen (CEA), carbohydrate antigen 125 (CA125), carbohydrate antigen 19-9 (CA19-9), cytokeratin fragment 21-1 (CYFRA21-1), CD59 glycoprotein, transthyretin (TTR), GM2 activator protein (GM2AP), haptoglobin-R 2, Ig-free light chain, neuron-specific enolase (NSE), nitrated ceruloplasmin, plasma kallikrein B1, ProGRP, retinol binding protein (RBP), squamous cell carcinoma (SCC), vascular endothelial growth factor (VEGF), TPA, tumor M2-pyruvate kinase, ENO1, Neuroendocrine markers, HER2, TAG-72.3, hnRNP-A2/B1, PCNA, CD34, c-erbB2, FHIT, CTNNB1, MUC1, Cyclin D1
Gene biomarkers	p53, p16, K-ras, microRNAs, miR-21, miR-210, miR-182, miR-31, miR-200b, miR-205, miR-183, miR-126-3p, miR-30a, miR-30d, miR-486-5p, miR-451a, miR-126-5p, miR-143, miR-145, miR-206, miR-133b, hsa-mir-155, hsa-let-7a-2, TERT, TERF2, POT1, MiR-449c

Table 2. Lung cancer markers.

demonstrates the current available biomarkers for lung cancer detection [15–35]. DNA biomarkers provide useful information on the process of tumor growth but they are insufficient sensitivity to detect early-stage tumors due to low concentrations of cancer markers [36]. Protein biomarkers are the major indicator of lung cancer, which can be classified as predictive and prognostic markers [37]. Predictive protein markers provide information of the particular therapeutic intervention, while prognostic protein markers offer the overall information of the subjects.

2.1. Proteomic biomarkers

Carcinoembryonic antigen (CEA) is the most common proteomic biomarker to distinguish malignant and benign tissues. Normally, serum level of CEA is about 2.5–5 ng/mL in healthy subjects [36]. Neuron-specific enolase (NSE) is a useful marker to investigate neuronal differentiation and to visualize the entire nervous and neuroendocrine systems. It exhibits calcium-dependent manner to perform its functions and needs magnesium as a cofactor for catalysis and stabilization of the dimer. Serum levels of NSE are related to some diseases such as Alzheimer, Huntington's chorea, neuroblastoma, and small cell lung cancer (SCLC). Compared to CEA, NSE is more sensitive and specific serum marker for SCLC [37]. Serum levels of NSE is higher than 9 ng/mL in patients with lung cancer. The subjects are considered with SCLS if the levels of NSE are higher than 35 ng/mL. The combination of NSE with other markers such as CYFRA 21-1 and CEA offered more effective and reliable detection in univariate and multivariate analysis of lung cancers.

Annexin II and enolase 1 (ENO1) are another common lung cancer biomarkers [38]. Chromogranin A (CgA) is an acidic glycoprotein, which belongs to the granin family of neuroendocrine secretory proteins. The threshold level of CgA is 50 ng/mL in patients with lung cancer. The serum levels of CgA were much higher in SCLC patients than that in the control groups, and there was an association between survival time and serum levels of CgA [39]. SCLC patients observed the best responses, but the percentage of this histological type composes of only 20% of all patients with lung cancer.

Cytokeratin-19 is the smallest human cytokeratin, which has been recommended as a high sensitive and specific marker for lung cancer, particularly in NSCLS. All adenocarcinomas tested have been positive for CYFRA 21-1, which was about 80% of patients with lung cancers [40]. The specificity and sensitivity of CYFRA 21-1 was found higher than the other protein markers such

as CEA and squamous cell carcinoma (SCC) to evaluate NSCLS. The combination of CYFRA 21-1 and other proteomic markers could increase the positive results of lung cancers [41].

However, it is difficult to detect lung cancer with the present markers because they are nonspecific indicators. To improve the accurate, many researchers have investigated the protein biomarker panel that consists of CEA, retinol binding protein (RBP), R1-antitrypsin (AAT), and squamous cell carcinoma (SCC) antigen for accurate disease detection [42]. The sensitivity was also improved by the biomarker panel consists of CEA and some specific biomarkers such as ENO1, SCC, NSE, CYFRA21-1 [43].

2.2. Gene biomarkers

The p53 protein is not normally detected in healthy lung tissue. Approximately 50% of NSCLC patients have been reported with p53 mutation, and the spectrum changed between 34% and 82%. p53 expression was observed in about 58% of lung cancer patients [44]. In addition, the poor correlation relationship between bcl-2 and p53 over-expression was observed in lung cancer patients [45].

p16 methylation was detected in lung cancer patients, in particularly, in chromate lung cancers and smokers. p16 methylation was found in approximately 21~51% of NSCLC patients, while p16 loss of heterozygosity was observed in about 54~100% of NSCLC patients [46, 47].

Ras genes are responsible for the cancer-causing activities of the Harvey (H-ras) and Kirsten (K-ras) sarcoma viruses. Ras mutations were discovered in lung cancer patients (20~25%) and patients with specific cancers (up to 90%). Approximately 60% of Ras mutations were confined to codon 12 of K-ras [48]. K-Ras mutation was also discovered in lung cancer patients (up to 78%) and in patients with NSCLS, pleural effusion, sputum, serum, and bronchoalveolar lavage fluid [49]. Some telomere-related genes such as telomerase reverse transcriptase (TERT), telomerase-associated factor 2 (TERF2) and protection of telomeres 1 (POT1) are affected on lung diseases [50, 51]. The telomeres are the territories of repetitive DNA that exist at the end of the chromosomes and are responsible for the protection of the chromosome ends.

Tumor growth is associated with silence and overexpression miRNAs, thus overexpress miRNAs has potential to become a useful clinical diagnostic tool for early lung diseases detection [52]. Seven upregulated (miR-21, miR-210, miR-182, miR-31, miR-200b, miR-205 and miR-183) and eight downregulated (miR-126-3p, miR-30a, miR-30d, miR-486-5p, miR-451a, miR-126-5p, miR-143 and miR-145) miRNAs have been investigated for lung marker detection [53]. Additionally, serum miR-206 and miR-133b have been considered as potential markers for lung carcinogenesis [51]. High hsa-mir-155 and low hsa-let-7a-2 can detect lung cancer correctly [54]. MiR-449c with the target marker c-Myc has been applied for NSCLS, which could suppress cancer cells growth in vivo [55].

3. Biosensors for lung cancer biomarker detection

Table 3 shows some recent developed biosensors for detecting lung tumor markers [56–72]. Fluorescence, interferometric, surface plasmon resonance biosensors (SPR), optrode-based

Biomarker	Capture agent	Sample	Transducer	Limit of detection	Linear range	Refs.
VEGF	VEGFreceptor-1	Serum	Electrochemical	-	10–70 pg/mL	[56]
	Aptamer	-	Electrochemical	15 nM	-	[57]
VEGF165	Aptamer	Serum	Fluorescent	-	1.25 pM–1.25 μM	[58]
LAG3 protein	Antibody	Plasma	SPRi-MALDITOP MS	-	-	[59]
TP53 gene	DNA		SPR and QCM	-	0.3–2 μM	[60]
COX-2	Polyclona antibody	Simulated blood sample	SPR	1.35×10^{-4} ng/mL	$3.64x10^{-4}$ – $3.64x10^{2}$ ng/mL	[61]
			Fluorescence	1.02×10^{-4} ng/mL	$7.46x10^{-4}$ – 7.46x10 ng/mL	
CEA	Antibody	Serum	SPR	-	-	[62]
p53 antibody	p53 antigen	Serum	Microcantilever biosensor	-	20 ng/mL–20 μg/mL	[63]
p53	ssDNA	-	Electrochemiluminescence	-	-	[64]
p53 (wild & total)	ds-DNA & antibody	-	SPR	10.6 and 1.06 pM	-	[65]
EGFR	Aptamer	Serum	Optical	-	-	[66]
CA 19-9	Antibody	-	SPR	66.7 U/mL	-	[67]
ALCAM	Antibody	10% Serum	SPRi	6 ng/mL	-	[68]
ALCAM & hCG	antibody	10%Serum	SPRi	45–100 ng/mL		[69]
TAGLN2	Antibody	10%Serum	SPRi	3 ng/mL		[70]
DNA mutations	ssDNA	Serum	SPR	50 nM		[71]
K-ras point mutation	PNA	-	SPR	-		[72]

Table 3. The recently developed biosensors for target lung tumor markers detection.

fiber, evanescent wave fiber, and resonant mirror biosensors are the main types of optical biosensors. SPR-based sensors are more attractive for lung cancer markers detection, which can be classified as label-free and real-time affinity reaction detection systems. A high-precision optical system was developed to detect CYFRA21-1 based on magnetic enzyme-linked immunoassay [73]. Experimental results demonstrated that the proposed optical system has potential to become a powerful tool for rapid diagnostic of lung cancer marker with several advantages such as compactness, sensitive, and fast. A plasmonic optical fiber immunosensor was also developed by Ribaut et al. to detect cytokeratin [74]. Their research findings offered an important milestone towards the clinical detection of biomarkers in tissues.

Quartz is a popular crystal to develop analytic devices such as quartz crystal microbalance (QCM) sensor. QCM-based sensors can detect point mutation in lung cancer patients [75], which measure frequency changes in quartz crystal resonators based on adsorbate recognition,

and the mass changes caused by selective binding can be detected by the corresponding changes in crystals. The advantages of piezoelectric sensors include easy-to-use, cost-effective, and sensitive.

Electrochemical biosensors measure the changes of dielectric properties, dimension, shape and charge distribution while antibody–antigen complex occurred on the electrode surface [76]. Electrochemical biosensors offer high sensitivity and specificity for lung tumor markers detection. Electrochemical-based transducers generally consists of semiconductors and screen-printed electrodes for constructing the biosensors, which able to detect molecules such as proteins, antibody, DNA, antigen and heavy metal ions. The recent advances in electrochemical nano-biosensors offer promising for diagnosis of molecules with significant benefits in inexpensive, simplicity, reliability and fast-response, high sensitivity and specificity.

4. Electromagnetic inductance tomography for lung cancer detection

Electromagnetic tomography (EMT) has attracted many attentions worldwide since it offers a promising alternative to existing medical imaging methods, such as CT or MRI. The approach uses non-ionizing radiation in the low GHz region of the EM spectrum. EMT approach is a safe and cost-effective diagnostic tool and provides structural and functional imaging in one device. Various EMT approaches have been applied for biomedical imaging with particular focus on imaging lung, brain, heart, liver tissue and biological tissues [77–90]. **Table 4** presents some recently developed EMT systems.

Watson et al. [91] developed an EMT with phase-stable amplifier for biomedical application. The phase-stable amplifiers and the gradiometers configurations need not be mutually exclusive, and it was reported that the highest measurement precision could be achieved by utilizing both approaches. The EMT image quality would be improved by increasing the number of transmitters and receivers, however, such method also increases the cost, complexity and operation time of the EMT system. A rotational EMT system containing a transceiver RF coil was developed for biomedical application. Compared to the conventional systems, the proposed rotational system offered a better field penetration depth towards the center of image.

Semenov et al. [92] investigated the ability of EMT technology to detect brain stroke within a human head phantom (see **Figure 1**). The FDTD method was applied to solve the 3D

	Frequency	Sampling rate	Driving level	Phase noise (m^o)	Phase drift (m^o)	Linearity
Bath Medical system	10 MHz	100MS/s	30 mA	4	25	$R^2 = 0.9996$
Cardiff Mk2 system [82, 83]	10 MHz	120MS/s	100mArms	9	119	$R^2 = 0.9998$
Craz Mk2 system [84]	50 kHz~ 1.5 MHz	60M/s	Max. 200 mA	N/A	N/A	N/A
Glamorgan system [85]	10 MHz	N/A	N/A	N/A	27	N/A
Phillips system [81]	10 MHz	192kS/s	50mArms	12.5	102	$R^2 = 0.9878$

Table 4. Some recently developed EMT systems.

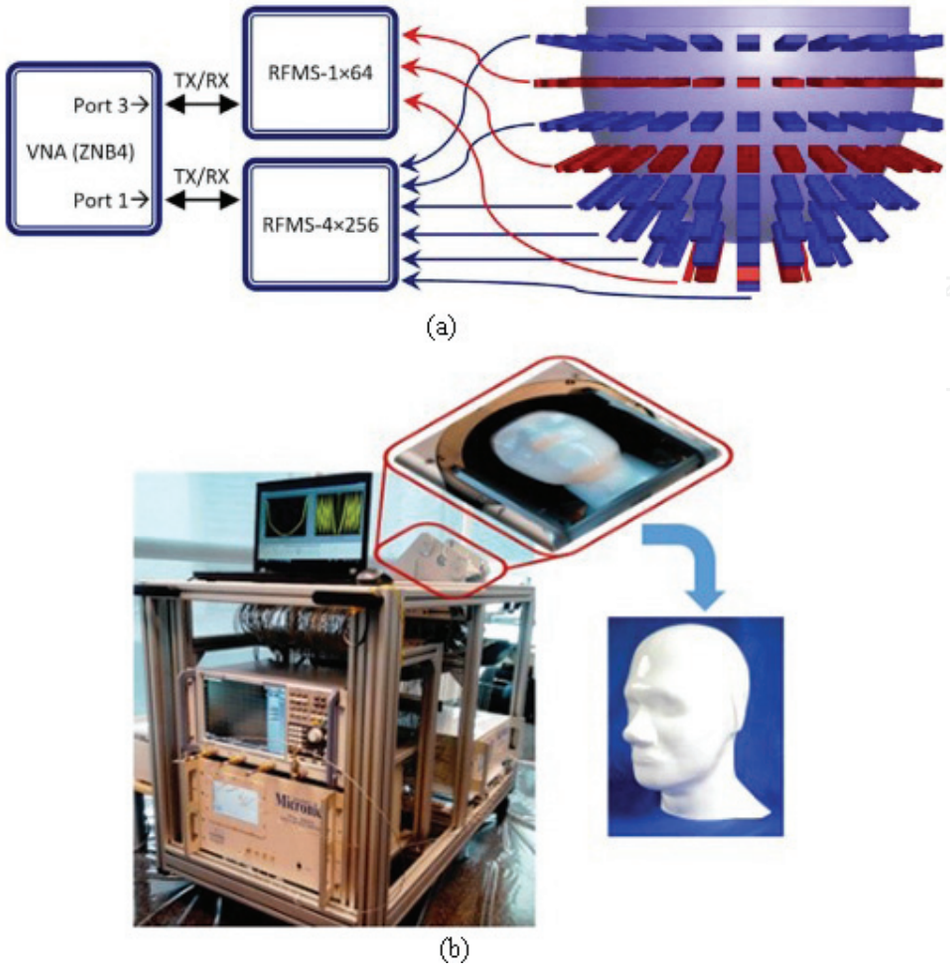

Figure 1. (**a**) The EMT system developed by Semenov et al. [92]; (**b**) a photograph of the EMT experimental setup using a head phantom for the imaging experiment.

electromagnetic problem, and the gradient-based approach was used to solve the inverse problem. The reconstructed images of head phantom are displayed in **Figure 2**. Their research findings demonstrated that EMT approach has the potential to become a useful tool for brain stroke detection in the future.

More recently, Wang et al. [93] proposed a single frequency EMT based approach for small lung tumor detection in human thorax models. As shown in **Figure 3**, the system made of 16 coils and each of them worked as both transmitter and receiver. The thorax model was located in the middle of the tank and was energized with a magnetic field generated by coils located outside of the tank wall. During data collection, the transmitting coils transmitted EM signals into the thorax, and the receiving coils measured the scattered magnetic fields from the thorax. A reconstructed image of the thorax model was obtained using the measured data.

Referring to **Figure 3**, if a point Q is located within the thorax model, the complex visibility data for any two coils can be obtained as [94]:

$$\overrightarrow{V_{i,j}} = < \vec{H}_{scat}\left(\vec{r}_i\right) \cdot \vec{H}^{*}_{scat}\left(\vec{r}_j\right) > \tag{1}$$

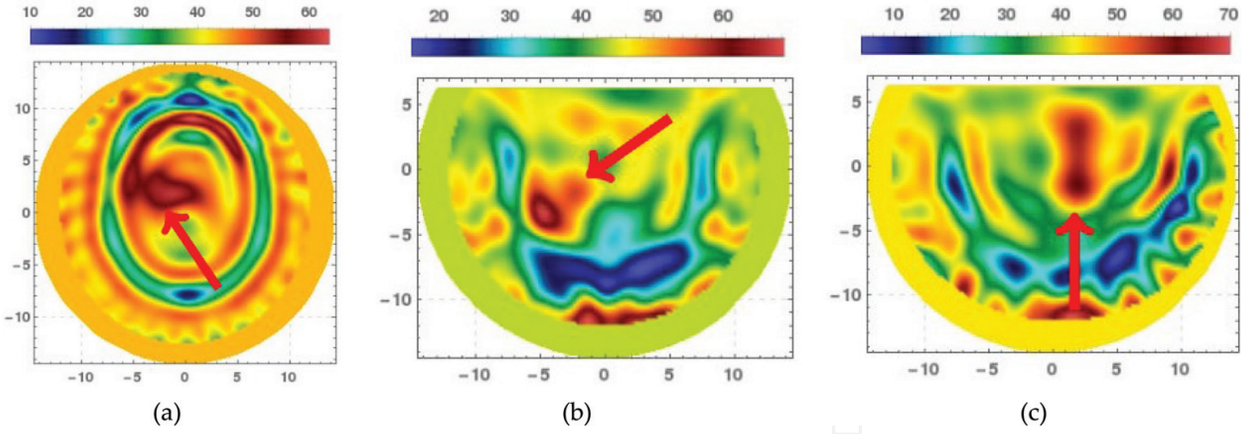

Figure 2. 3D reconstruction of the human head phantom featuring a h-stroke model. Three slices of the real part of the 3D ε-distribution, (**a**) axial slice; (**b**) coronal slice; (**c**) sagittal slice [92].

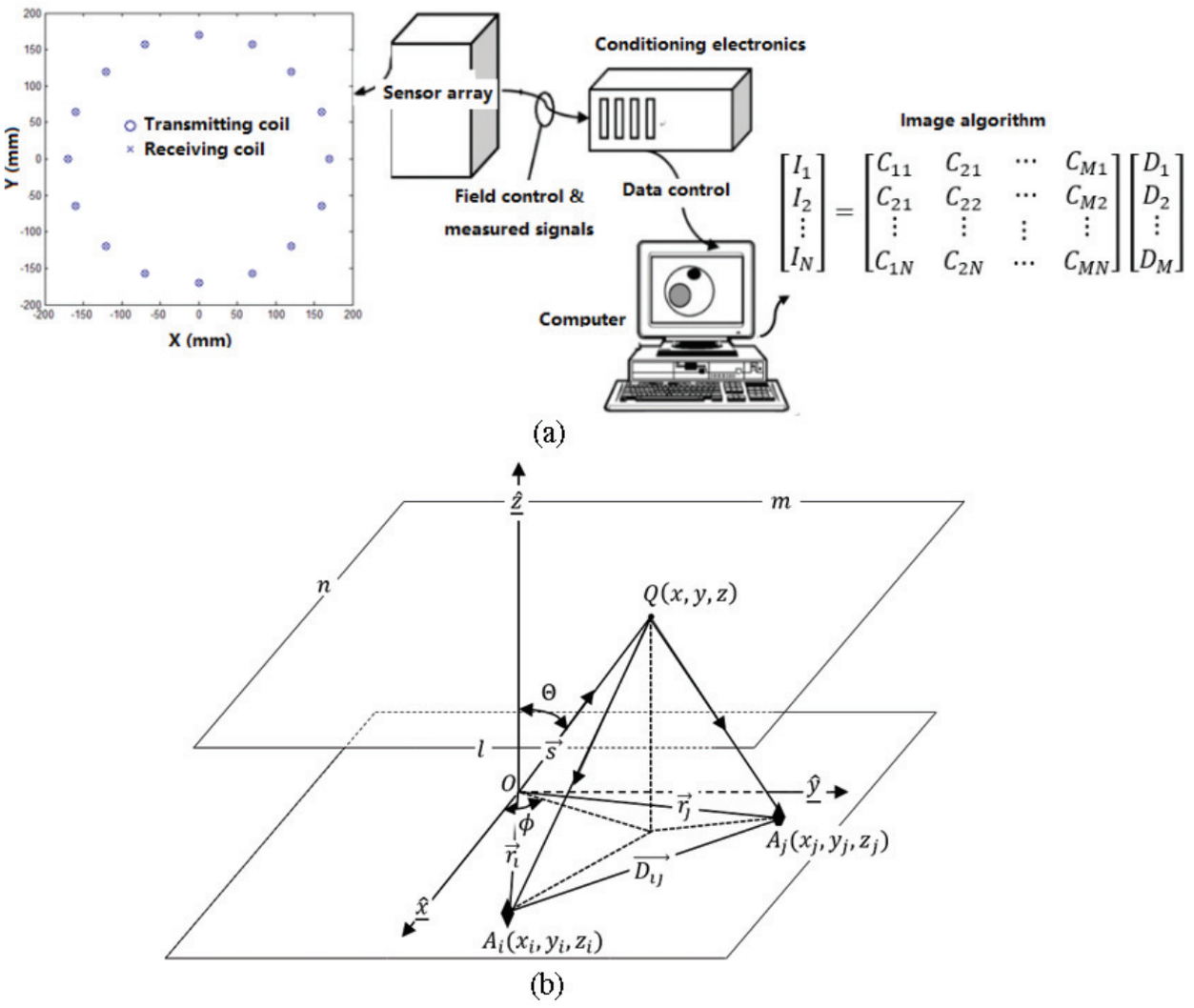

Figure 3. (**a**) The proposed EMT system by Wang et al. [93]; (**b**) a setup for any pair of coils.

Where $\vec{r}_i$ and $\vec{r}_j$ denote the coil locations, <> means the time average, **Table 3** lists all symbols and abbreviations. The total complex visibility data of N coils is $\vec{V} = \sum_i^N \overrightarrow{V_{i,j}}$, $N \geq 3, i \neq j$.

Define the intensity of thorax as:

$$I\left(\vec{s}\right) = \left(\frac{j\omega\mu_0}{4\pi}\right)^2 \left|\sigma(s) + j\omega\varepsilon_0\varepsilon_r'\right|^2 \overrightarrow{H_T}\left(\vec{s}\right) \cdot \overrightarrow{H_T^*}\left(\vec{s}'\right) \tag{2}$$

If all coils located at the same height, then a 2D image can be reconstructed:

$$\tilde{I}(l,m) = \iint V(u,v) e^{j2\pi\left(u_{ij}l + v_{ij}m\right)} du dv \tag{3}$$

Where $l = sin\theta cos\phi$ and $m = sin\theta sin\phi$, $u_{ij} = \left(\vec{x_j} - \vec{x_i}\right)/\lambda_0$ and $v_{ij} = \left(\vec{y_j} - \vec{y_i}\right)/\lambda_0$, λ_0 indicates the wavelength of free space (see **Figure 3**).

To study the feasibility of EMT for lung tumor detection, Wang et al. developed a numerical system using MATLAB software. The system made of 16 circular coils. The electric current density generated from transmitter was 1A/m^2. The finite element approach was applied to compute the voltage and the measured region was divided into triangular meshes. The working frequency was 2 MHz. The excitation current density $\vec{J_s}$ was simulated by:

$$\vec{J_s} = \nabla \times \left(\mu_0^{-1} \nabla \times \vec{A}\right) + j\omega\sigma \vec{A} \tag{4}$$

Eq. (4) can be rewritten from Maxwell's formulas by calculating the total electric field $\vec{E} = j\omega \vec{A} - \nabla\Omega$.

The scattered field measured by any receiver can be modeled as [95]:

$$\vec{H}_{scat}\left(\vec{r_0}\right) = \frac{-j}{4\pi\omega\mu_0} \int_V \left[\left(\vec{J_s} \cdot \nabla\right) \times \nabla + k_0^2 \vec{J_M} + j\omega\mu_0 \vec{J_S} \nabla\right] G\left(\vec{r}, \vec{r_0}\right) dV \tag{5}$$

Where $\vec{J_s} = j\omega\varepsilon_0(\varepsilon_r - 1)\ \vec{E}$, $\overrightarrow{J_M} = j\omega\mu_0\left(\mu_r - 1\right)\ \overrightarrow{H_T}$, $\overrightarrow{H_T} = \vec{H}_{inc} + \vec{H}_{scat}$.

The following formula can be applied to compute the magnetic field:

$$\vec{H}_{scat}\left(\vec{r_0}\right) = \frac{k_0^2}{4\pi} \int_V \left[\left(a\ \vec{H} + b\left(\vec{H} \cdot \hat{\underline{r}}\right)\hat{\underline{r}}\right] G\left(\hat{r}, \vec{r_0}\right) dV \tag{6}$$

Where $a = \mu_r\varepsilon_r - \frac{j\left(\mu_r - 1\right)}{k_0 R}\left(1 - \frac{j}{k_0 R}\right)$, $b = \left(\mu_r - 1\right)\left(-1 + \frac{3j}{k_0 R} + \frac{3}{(k_0 R)^2}\right)$, a and b are proportional to $1/R^2$(i.e. $k_0 R \ll 1$). Hence $k_0^2 a \cong -\left(\mu_r - 1\right)/R^2$ and $k_0^2 b \cong 3\left(\mu_r - 1\right)/R^2$.

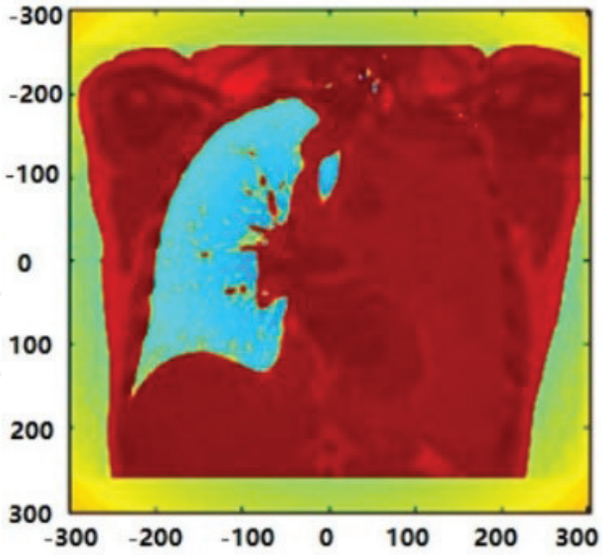

Figure 4. Simulation result of lung phantom obtained by Wang et al. [93].

Born Approximation was applied to solve the forward problem, thus Eq. (6) changes to [90]:

$$\vec{H}_{scat}\left(\vec{r_0}\right) = \frac{1}{4\pi}\int_V \frac{\mu_r - 1}{R^2}\left[-\vec{H} + 3\left(\vec{H}\cdot\underline{\hat{r}}\right)\underline{\hat{r}}\right] G\left(\vec{r}, \vec{r_0}\right) dV \tag{7}$$

Simulation result (see **Figure 4**) showed that various arbitrary shaped lung tumors with random sizes and locations could be identified in the thorax images. The proposed EMT approach offered crucial priority information that can be exploited to improve the capabilities of diagnostics methods. The advantages of the proposed method include simplified imaging processing due to the image quantity is proportional to the dielectric properties contrast.

5. Current trends and future perspectives

The current available lung screening approaches are effective but have some limitations as detailed above. EMT-based approaches have the potential to become an additional or alternative method to CT for lung disease detection. However, these techniques have some drawbacks, such as heavy computational imaging algorithm, difficult hardware systems for clinical applications, and limited spatial resolution. To solve these challenges, many researchers focused on developing a high dynamic hardware implementation system. Additionally, many investigators used more coils to improve the image quality. However, such method increases the mutual coupling signals between coils, which may reduce the detection accuracy. Moreover, the cost and complexities of the hardware implementation system also increased with increasing the number of coils. To solve this problem, a single coil could be applied to replace the multi-coil array. Recent research findings suggested that optimization of coil array configurations offer some potential benefits in high image resolution, low-cost, and operating time. The multiple-input-multiple-output technique may also help to reduce the complexity of the hardware system. In the future, more investigations of EMT technique should be taken to improve the image

algorithm and hardware implementation system with particular focus on the development of low-cost and compact RF coils and coil arrays to produce high quality images.

Developing biosensors with implementation of biomarkers have attracted many attentions from researchers worldwide in the past few years. Up to date, cancer markers are still in discovery stage and the current evidences are too restricted for early lung cancer detection. Proteomic biomarkers have been applied within a panel of protein biomarkers but they are not recommended to be used as individual biomarkers for lung cancer detection. Applying individual marker does not helpful for clinicians to obtain enough information of cancer tissue such as the stage of cancer, treatment and state of subject. The major problem of biosensor-based techniques is related to integration of lung cancer detection in primary healthcare. QCM-based biosensors are more suitable and reliable for clinical surgery compared to other biosensors. The limitations of biosensors include small target size, marker levels, the possibility of high non-specific binding in the case of serum or real patient samples. Recent research trends of nano-biosensor techniques for diagnosis of molecules offer great potential for early lung cancer detection, however, these techniques are not mature for clinical trials. Future investigations should be address directly to improve the selectivity, sensitivity, accuracy, and multiplexing capacity of biosensors.

Acknowledgements

The author gratefully acknowledges the financial supports from the National Natural Science Foundation of China (Grant No. 61701159), the Natural Science Foundation of Anhui Province (Grant No. 101413246), the Foundation for Oversea Master Project from Ministry of Education of the People's Republic of China (Grant No. 2160311028), and the start-up funding from the Hefei University of Technology (Grant No. 407037164).

Author details

Lulu Wang[1,2]* and Jinzhang Xu[3]

*Address all correspondence to: luluwang2015@hfut.edu.cn

1 School of Instrument Science and Opto-electronics Engineering, Hefei University of Technology, Hefei, China

2 Institute of Biomedical Technologies, Auckland University of Technology, Auckland, New Zealand

3 School of Electrical Engineering and Automation, Hefei University of Technology, Hefei, China

References

[1] World Health Organization. Cancer fact sheet 2017. Available at: http://www.who.int/mediacentre/factsheets/fs297/en/ [Accessed 22.09.2017.]

[2] Reed MF, Molloy M, Dalton EL, Howington JA. Survival after resection for lung cancer is the outcome that matters. American Journal of Surgery. 2004;**188**(5):598-602

[3] Chiang TA, Chen PH, PF W, Wang TN, Chang PY, Ko AM, Huang MS, Ko YC. Important prognostic factors for the long-term survival of lung cancer subjects in Taiwan. BMC Cancer. 2008;**8**(1):324

[4] Journy N, Rehel JL, Pointe HDL, Lee C, Brisse H, Chateil JF, et al. Are the studies on cancer risk from CT scans biased by indication|[quest]| elements of answer from a large-scale cohort study in France. British Journal of Cancer. 2015;**112**(11):1841-1842

[5] Aberle DR, Adams AM, Berg CD, Black WC, Clapp JD, Fagerstrom RM, Gareen IF, Gatsonis C, Marcus PM, Sicks JD, et al. Reduced lung-cancer mortality with low-dose computed tomographic screening. The New England Journal of Medicine. 2011;**365**:395-409

[6] Asselin MC, O'Connor JPB, Boellaard R, Thacker NA, Jackson A. Quantifying heterogeneity in human tumours using MRI and PET. European Journal of Cancer. 2012;**48**:447-455

[7] Chicklore S, Goh V, Siddique M, Roy A, Marsden PK, Cook GJR. Quantifying tumour heterogeneity in F-18-FDG PET/CT imaging by texture analysis. European Journal of Nuclear Medicine and Molecular Imaging. 2013;**40**:133-140

[8] Ippolito D, Capraro C, Guerra L, De Ponti E, Messa C, Sironi S. Feasibility of perfusion CT technique integrated into conventional (18) FDG/PET-CT studies in lung cancer patients: Clinical staging and functional information in a single study. European Journal of Nuclear Medicine and Molecular Imaging. 2013;**40**:156-165

[9] Ghosal R, Kloer P, Lewis KE. A review of novel biological tools used in screening for the early detection of lung cancer. Postgraduate Medical Journal. 2009;**85**(1005):358-363

[10] Griffiths H. Magnetic induction tomography. Measurement Science & Technology. 2011; **12**(8):1126-1131

[11] Cheng BY. Development of a chemiluminescent immunoassay for cancer antigen 15–3. Labeled Immunoass. Clinical Medicine. 2016;**23**:1348-1351

[12] Sone K, Oguri T, Nakao M, Kagawa Y, Kurowaka R, Furuta H, et al. Cyfra 21-1 as a predictive marker for non-small cell lung cancer treated with pemetrexed-based chemotherapy. Anticancer Research. 2017;**37**(2):935

[13] Wang L. Early diagnosis of breast cancer. Sensor. 2017;**17**:1572

[14] Zhang Y, Yang D, Weng L, Wang L. Early lung cancer diagnosis by biosensors. International Journal of Molecular Sciences. 2013;**14**(8):15479-15509

[15] Jia JW, Li KL, Wu JX, Guo SL. Clinical significance of annexin ii expression in human non-small cell lung cancer. Tumour Biology the Journal of the International Society for Oncodevelopmental Biology & Medicine. 2013;**34**(3):1767-1771

[16] Uribarri M, Hormaeche I, Zalacain R, Lopezvivanco G, Martinez A, Nagore D, et al. A new biomarker panel in bronchoalveolar lavage for an improved lung cancer diagnosis.

Journal of Thoracic Oncology Official Publication of the International Association for the Study of Lung Cancer. 2014;**9**(10):1504-1512

[17] Dong Y, Zheng X, Yang Z, Sun M, Zhang G, An X, et al. Serum carcinoembryonic antigen, neuron-specific enolase as biomarkers for diagnosis of nonsmall cell lung cancer. Journal of Cancer Research & Therapeutics. 2016;**12**:34

[18] Gube M, Taeger D, Weber DG, Pesch B, Brand P, Johnen G, et al. Performance of biomarkers smrp, ca125, and cyfra 21-1 as potential tumor markers for malignant mesothelioma and lung cancer in a cohort of workers formerly exposed to asbestos. Archives of Toxicology. 2011;**85**(3):185-192

[19] Huang Z, Jiang Z, Zhao C, Han W, Lin L, Liu A, et al. Simple and effective label-free electrochemical immunoassay for carbohydrate antigen 19-9 based on polythionine-au composites as enhanced sensing signals for detecting different clinical samples. International Journal of Nanomedicine. 2017;**12**:3049-3058

[20] So HJ, Hong SI, Lee JK, Chang YH, Kang SJ, Hong YJ. Comparison of the serum fibrin-fibrinogen degradation products with cytokeratin 19 fragment as biomarkers in patients with lung cancer. Biomedical Reports. 2014;**2**(5):737-742

[21] Li B, Lin H, Fan J, Lan J, Zhong Y, Yang Y, et al. Cd59 is overexpressed in human lung cancer and regulates apoptosis of human lung cancer cells. International Journal of Oncology. 2013;**43**(3):850-858

[22] Ding H, Liu J, Xue R, Zhao P, Qin Y, Zheng F, et al. Transthyretin as a potential biomarker for the differential diagnosis between lung cancer and lung infection. Biomedical Reports. 2014;**2**(5):765

[23] Potprommanee L, Ma HT, Shank L, Juan YH, Liao WY, Chen ST, et al. Gm2-activator protein: A new biomarker for lung cancer. Journal of Thoracic Oncology. 2015;**10**(1):102-109

[24] Wang B, He YJ, Tian YX, Yang RN, Zhu YR, Qiu H. Clinical utility of haptoglobin in combination with cea, nse and cyfra21-1 for diagnosis of lung cancer. Asian Pacific Journal of Cancer Prevention. 2014;**15**(22):9611-9614

[25] Kormelink TG, Powe DG, Kuijpers SA, Abudukelimu A, Fens MHAM, Pieters EHE, et al. Immunoglobulin free light chains are biomarkers of poor prognosis in basal-like breast cancer and are potential targets in tumor-associated inflammation. Oncotarget. 2014;**5**(10):3159-3167

[26] Zhou Y, Chen WZ, Peng AF, Tong WL, Liu JM, Liu ZL. Neuron-specific enolase, histopathological types, and age as risk factors for bone metastases in lung cancer. Tumour Biology the Journal of the International Society for Oncodevelopmental Biology & Medicine. 2017;**39**(7):1010428317714194

[27] Martin Mateo MC, Bustamante BJ, Font AI. Serum copper, ceruloplasmin, lactic-dehydrogenase and alpha 2-globulin in lung cancer. Biomedicine/[publiée pour l'A.A.I.C.I.G.]. 1979; **31**(3):66-68

[28] Chee J, Naran A, Misso NL, Thompson PJ, Bhoola KD. Expression of tissue and plasma kallikreins and kinin b1 and b2 receptors in lung cancer. Biological Chemistry. 2008;**389**(9): 1225-1233

[29] Winther B, Reubsaet JL. Determination of the small cell lung cancer associated biomarker pro-gastrin-releasing peptide (progrp) using lc-ms. Journal of Separation Science. 2015;**30**(2): 234-240

[30] Wang T, Liang Y, Thakur A, Zhang S, Liu F, Khan H, et al. Expression and clinicopathological significance of s100 calcium binding protein a2 in lung cancer patients of chinese han ethnicity. Clinica Chimica Acta. 2017;**464**:118-122

[31] Wang T, Zhang L, Tian P, Tian S. Identification of differentially-expressed genes between early-stage adenocarcinoma and squamous cell carcinoma lung cancer using meta-analysis methods. Oncology Letters. 2017;**13**(5):3314

[32] Loftus TJ, Thomson AJ, Kannan KB, Alamo IG, Ramos HN, Whitley EE, et al. Effects of trauma, hemorrhagic shock, and chronic stress on lung vascular endothelial growth factor. Journal of Surgical Research. 2017;**210**:15

[33] Foa P, Fornier M, Miceli R, Seregni E, Santambrogio L, Nosotti M, et al. Tumour markers cea, nse, scc, tpa and cyfra 21.1 in resectable non-small cell lung cancer. Anticancer Research. 1999;**19**(4C):3613

[34] Liu J, Zhu H, Jiang H, Zhang H, Wu D, Hu X, et al. Tumor m2 pyruvate kinase in diagnosis of nonsmall cell lung cancer: A meta-analysis based on Chinese population. Journal of Cancer Research & Therapeutics. 2015;**11**(5):c104

[35] Indovina P, Marcelli E, Pentimalli F, Tanganelli P, Tarro G, Giordano A. Mass spectrometry-based proteomics: The road to lung cancer biomarker discovery. Mass Spectrometry Reviews. 2013;**32**(2):129-142

[36] Ye F, Shi MY, Zhao S. Noncompetitive immunoassay for carcinoembryonic antigen in human serum by microchip electrophoresis for cancer diagnosis. Clinica Chimica Acta. 2010;**411**:1058

[37] Schneider J, Philipp MVelcovsky HG, Morr H, Katz N. Pro-gastrin-releasing peptide (progrp), neuron specific enolase (NSE), carcinoembryonic antigen (CEA) and cytokeratin 19-fragments (cyfra 21-1) in patients with lung cancer in comparison to other lung diseases. Anticancer Research. 2003;**23**(2A):885

[38] Ho JA, Chang HC, Shih NY, Wu LC, Chang YF, Chen CC, et al. Diagnostic detection of human lung cancer-associated antigen using a gold nanoparticle-based electrochemical immunosensor. Analytical Chemistry. 2010;**82**(14):5944-5950

[39] Songnan Q, Mo H, Huan T, Yudong L, Min J, Lin W, et al. Autoantibodies to chromogranin a are potential diagnostic biomarkers for non-small cell lung cancer. Tumor Biology. 2015;**36**(12):9979-9985

[40] Holdenrieder S, Wehnl B, Hettwer K, Simon K, Uhlig S, Dayyani F. Carcinoembryonic antigen and cytokeratin-19 fragments for assessment of therapy response in non-small cell lung cancer: A systematic review and meta-analysis. British Journal of Cancer. 2017; **116**(8):1037

[41] Chu XY, Hou XB, Song WA, Xue ZQ, Wang B, Zhang LB. Diagnostic values of scc, cea, cyfra21-1 and nse for lung cancer in patients with suspicious pulmonary masses: A single center analysis. Cancer Biology & Therapy. 2011;**11**(12):995-1000

[42] Jr PE, Campa MJ, Gottlin EB, Kusmartseva I, Guan XR, Nd HJ. Panel of serum biomarkers for the diagnosis of lung cancer. Journal of Clinical Oncology Official Journal of the American Society of Clinical Oncology. 2007;**25**(35):5578

[43] Bennett WP, Hussain SP, Vahakangas KH, Khan MA, Shields PG, Harris CC. Molecular epidemiology of human cancer risk: Gene–environment interactions and p53 mutation spectrum in human lung cancer. Journal of Pathology. 1999;**187**(1):8-18

[44] Zereu M, Vinholes JJ, Zettler CG. P53 and bcl-2 protein expression and its relationship with prognosis in small-cell lung cancer. Clinical Lung Cancer. 2003;**4**(5):298-302

[45] Kim DH, Nelson HH, Wiencke JK, Zheng S, Christiani DC, Wain JC, et al. P16(ink4a) and histology-specific methylation of cpg islands by exposure to tobacco smoke in non-small cell lung cancer. Cancer Research. 2001;**61**(8):3419-3424

[46] Kondo K, Takahashi Y, Hirose Y, Nagao T, Tsuyuguchi M, Hashimoto M, et al. The reduced expression and aberrant methylation of p16(ink4a) in chromate workers with lung cancer. Lung Cancer. 2006;**53**(3):295

[47] Belinsky SA, Klinge DM, Liechty KC, March TH, Kang T, Gilliland FD, et al. Plutonium targets the p16 gene for inactivation by promoter hypermethylation in human lung adenocarcinoma. Carcinogenesis. 2004;**25**(6):1063

[48] Kovalchuk O, Naumnik W, Serwicka A, Chyczewska E, Niklinski J, Chyczewski L. K-ras codon 12 mutations may be detected in serum of patients suffering from adeno- and large cell lung carcinoma. A preliminary report. Folia Histochemica et Cytobiologica. 2001;**39**:70

[49] Iii HH, Cawthon R, He X, Chanock S, Lan Q. Genetic variation in telomere maintenance genes, telomere length, and lung cancer susceptibility. Lung Cancer. 2009;**66**(2):157-161

[50] Hu Z, Yang Z, Tian T, Liang J, Jin G, Shen H. Association between microrna polymorphisms, expressions, lung cancer development and prognosis. Biomedicine & Pharmacotherapy. 2009;**63**:322

[51] Schmitt MJ, Margue C, Behrmann I, Kreis S. Mirna-29: A microrna family with tumor-suppressing and immune-modulating properties. Current Molecular Medicine. 2013;**13**: 572-585

[52] Dacic S. Molecular prognostic markers of lung cancer. In: Molecular Pathology of Lung Cancer. New York: Springer; 2012

[53] JJ W, Yang T, Li X, Yang QY, Liu R, Huang JK, Li YQ, Yang CF, Jiang YG. Alteration of serum mir-206 and mir-133b is associated with lung carcinogenesis induced by 4-(methylnitrosamino)-1-(3-pyridyl)-1-butanone. Toxicology and Applied Pharmacology. 2013;**267**:238-2463

[54] Yanaihara N, Caplen N, Bowman E, Seike M, Kumamoto K, Yi M, et al. Unique microrna molecular profiles in lung cancer diagnosis and prognosis. Cancer Cell. 2006;**9**(3):189-198

[55] Miao LJ, Huang SF, Sun ZT, Gao ZY, Zhang RX, Liu Y, Wang J. Mir-449c targets C-myc and inhibits nsclc cell progression. FEBS Letters. 2013;**587**:1359-1365

[56] Sezginturk MK. A new impedimetric biosensor utilizing vegf receptor-1 (flt-1): Early diagnosis of vascular endothelial growth factor in breast cancer. Biosensors & Bioelectronics. 2011;**26**:4032-4039

[57] Nonaka Y, Abe K, Ikebukuro K. Electrochemical detection of vascular endothelial growth factor with aptamer sandwich. Electrochemistry. 2012;**80**:363-366

[58] Cho H, Yeh EC, Sinha R, Laurence TA, Bearinger JP, Lee LP. Single-step nanoplasmonic vegf(165) aptasensor for early cancer diagnosis. ACS Nano. 2012;**6**:7607-7614

[59] Remy-Martin F, El Osta M, Lucchi G, Zeggari R, Leblois T, Bellon S, Ducoroy P, Boireau W. Surface plasmon resonance imaging in arrays coupled with mass spectrometry (supra-ms): Proof of concept of on-chip characterization of a potential breast cancer marker in human plasma. Analytical and Bioanalytical Chemistry. 2012;**404**:423-432

[60] Altintas Z, Uludag Y, Gurbuz Y, Tothill IE. Surface plasmon resonance based immunosensor for the detection of the cancer biomarker carcinoembryonic antigen. Talanta. 2011;**86**:377-383

[61] Noah NM, Mwilu SK, Sadik OA, Fatah AA, Arcilesi RD. Immunosensors for quantifying cyclooxygenase 2 pain biomarkers. Clinica Chimica Acta. 2011;**412**:1391-1398

[62] Ladd J, Lu H, Taylor AD, Goodell V, Disis ML, Jiang S. Direct detection of carcinoembryonic antigen autoantibodies in clinical human serum samples using a surface plasmon resonance sensor. Colloids and Surfaces B. 2009;**70**:1-6

[63] Zhou Y, Wang Z, Yue W, Tang K, Ruan W, Zhang Q, Liu L. Label-free detection of p53 antibody using a microcantilever biosensor with piezoresistive readout. IEEE Sensors. 2009. DOI: 10.1109/ICSENS.2009.5398558

[64] Wang X, Zhang X, He P, Fang Y. Sensitive detection of p53 tumor suppressor gene using an enzyme-based solid-state electrochemiluminescence sensing platform. Biosensors & Bioelectronics. 2011;**26**:3608-3613

[65] Wang Y, Zhu X, Wu M, Xia N, Wang J, Zhou F. Simultaneous and label-free determination of wild-type and mutant p53 at a single surface plasmon resonance chip preimmobilized with consensus dna and monoclonal antibody. Analytical Chemistry. 2009;**81**:8441-8446

[66] Ilyas A, Asghar W, Allen PB, Duhon H, Ellington AD, Iqbal SM. Electrical detection of cancer biomarker using aptamers with nanogap break-junctions. Nanotechnology. 2012;**23**. DOI: 10.1088/0957-4484/23/27/275502

[67] Chung JW, Bernhardt R, Pyun JC. Additive assay of cancer marker ca 19–9 by spr biosensor. Sensors and Actuators B: Chemical. 2006;**118**:28-32

[68] Ladd J, Taylor AD, Piliarik M, Homola J, Jiang S. Label-free detection of cancer biomarker candidates using surface plasmon resonance imaging. Analytical and Bioanalytical Chemistry. 2009;**393**:1157-1163

[69] Yokotani T, Koizumi T, Taniguchi R, Nakagawa T, Isobe T, Yoshimura M, et al. Expression of α and β genes of human chorionic gonadotropin in lung cancer. International Journal of Cancer Journal International Du Cancer. 1997;**71**(4):539-544

[70] Piliarik M, Bockova M, Homola J. Surface plasmon resonance biosensor for parallelized detection of protein biomarkers in diluted blood plasma. Biosensors & Bioelectronics. 2010;**26**:1656-1661

[71] Carrascosa LG, Calle A, Lechuga LM. Label-free detection of DNA mutations by spr: Application to the early detection of inherited breast cancer. Analytical and Bioanalytical Chemistry. 2009;**393**:1173-1182

[72] Sato Y, Fujimoto K, Kawaguchi H. Detection of a k-ras point mutation employing peptide nucleic acid at the surface of a spr biosensor. Colloids and Surfaces B. 2003;**27**:23-31

[73] Piliarik M, Vaisocherova H, Homola J. Surface plasmon resonance biosensing. Methods in Molecular Biology. 2009;**503**:65-88

[74] Wang B, Liu JT, Luo JP, Wang MX, Shu-Xue QU, Cai XX. A three-channel high-precision optical detecting system for lung cancer marker cyfra21-1. Journal of Optoelectronics·Laser. 2013;**24**(9):1849-1854

[75] Ribaut C, Loyez M, Larrieu JC, Chevineau S, Lambert P, Remmelink M, Wattiez R, Christophe CC. Cancer biomarker sensing using packaged plasmonic optical fiber gratings: Towards in vivo diagnosis. Biosensors & Bioelectronics. 2016;**92**:449-456

[76] Sun W, Song W, Guo X, Wang Z. Ultrasensitive detection of nucleic acids and proteins using quartz crystal microbalance and surface plasmon resonance sensors based on target-triggering multiple signal amplification strategy. Analytica Chimica Acta. 2017;**978**:42

[77] Chen M, Hou C, Huo D, Yang M, Fa H. A highly sensitive electrochemical DNA biosensor for rapid detection of cyfra21-1, a marker of non-small cell lung cancer. Analytical Methods. 2015;**7**(22):9466-9473

[78] Marmugi L, Renzoni F. Optical magnetic induction tomography of the heart. Scientific Reports. 2016;**6**:23962

[79] Hu G, Cressman E, He B. Magnetoacoustic imaging of human liver tumor with magnetic induction. Applied Physics Letters. 2011;**98**(2):681

[80] Żywica AR. Magnetoacoustic tomography with magnetic induction for biological tissue imaging: Numerical modelling and simulations. Archives of Electrical Engineering. 2016; **65**(1):141-150

[81] Watson S, Williams RJ, Griffiths H, Gough W, Morris A. Magnetic induction tomography: Phase versus vector-voltmeter measurement techniques. Physiological Measurement. 2003;**24**(2):555

[82] Vauhkonen M, Hamsch M, Igney CH. A measurement system and image reconstruction in magnetic induction tomography. Physiological Measurement. 2008;**29**(6):S445

[83] Igney CH, Watson S, Williamson SJ, Griffiths H, Dössel O. Design and performance of a planar-array MIT system with normal sensor alignment. Physiological Measurement. 2005;**26**(2):S263-S278

[84] Patz R, Watson S, Ktistis C, Hamsch M, Peyton AJ. Performance of a FPGA-based direct digitising signal measurement module for MIT. Journal of Physics: Conference Series. 2010;**224**:1-4

[85] Scharfetter H, Kostinger A, Issa S. Hardware for quasi-single-shot multifrequency magnetic induction tomography (MIT): The Graz Mk2 system. Physiological Measurement. 2008;**29**:S431

[86] Wei H, Soleimani M. Electromagnetic tomography for medical and industrial applications: Challenges and opportunities. Proceedings of the IEEE. 2013;**101**(3):559-565

[87] Ma L, Soleimani M. Magnetic induction tomography methods and applications: A review. Measurement Science & Technology. 2017;**28**(7)

[88] Feldkamp JR, Quirk S. Optically tracked, single-coil, scanning magnetic induction tomography. Journal of Medical Imaging. 2017;**4**(2):023504

[89] Feldkamp JR. Single-coil magnetic induction tomographic three-dimensional imaging. Journal of Medical Imaging. 2015;**2**(1):013502

[90] Xiao Z, Tan C, Dong F. Effect of inter-tissue inductive coupling on multi-frequency imaging of intracranial hemorrhage by MIT. Measurement Science & Technology. 2017;**28**(8)

[91] Watson S, Wee HC, Griffiths H, Williams RJA. Highly phase-stable differential detector amplifier for magnetic induction tomography. Physiological Measurement. 2011;**32**:917

[92] Semenov S, Hopfer M, Planas R, Hamidipour A, Henriksson T. Electromagnetic tomography for brain imaging: 3D reconstruction of stroke in a human head phantom. IEEE Antenna Measurements & Applications. 2017:1-4

[93] Wang L, Al-Jumaily AM. Imaging of lung structure using holographic electromagnetic induction. IEEE Access. 2017;**PP**(99):1

[94] Wang L, Al-Jumaily AM, Simpkin R. Imaging of 3-D dielectric objects using far-field holographic microwave imaging technique. Progress in Electromagnetics Research B. 2014;**61**:135-147

[95] Levanda R, Leshem A. Synthetic aperture radio telescopes. IEEE Signal Process. 2010;**27**:14-29